Birefringence phase-matched direct third-harmonic generation in a ridge optical waveguide based on a KTiOPO4 single crystal

Augustin Vernay, Véronique Boutou, Corinne Félix, David Jegouso, Florent Bassignot, Mathieu Chauvet, Benoit Boulanger

HAL Id: hal-03436956

https://hal.science/hal-03436956

Submitted on 19 Nov 2021

Birefringence phase-matched direct third-harmonic generation in a ridge optical waveguide based on a KTiOPO$_4$ single crystal

Augustin Vernay,[1] **Véronique Boutou,**[1,4] **Corinne Félix,**[1] **David Jegouso,**[1] **Florent Bassignot,**[2] **Mathieu Chauvet,**[3] **and Benoit Boulanger**[1,5] (iD)

[1]*Univ. Grenoble Alpes, CNRS, Institut Néel, 38000 Grenoble, France*
[2]*Femto-Engineering, 15B avenue des Montboucons, 25000 Besançon, France*
[3] *FEMTO-ST Institute, UMR CNRS 6174, University of Bourgogne Franche-Comté, 15B avenue des Montboucons, 25000 Besançon, France*
[4]*veronique.boutou@neel.cnrs.fr*
[5]*benoit.boulanger@neel.cnrs.fr*

Abstract: Birefringence phase-matched third-harmonic generation at 1594 nm is performed for the first time in a KTiOPO$_4$ single crystal micrometric ridge waveguide. The energy conversion efficiency reaches 3.4% for a pump energy as low as 2 µJ over a pulse duration of 15 ps at a repetition rate of 10 Hz. Strong agreements between theory and experiments for both phase-matching and conversion efficiency is obtained, which let us envision future triple photon generation quantum experiments.

1. Introduction

Beside efficient generation of short wavelengths, nonlinear Third-Harmonic Generation (THG) components also have the thrilling potential for novel quantum optical experiments based on direct Triple Photons Generation (TPG) [1,2]. The biaxial nonlinear crystal KTiOPO$_4$ (KTP) is of prime interest in this quantum framework, including Second-Order spontaneous down-conversion [3]. Note also that the quest for compact, efficient and fiber compatible THG devices is thus still a hot topic.

THG can be achieved in a direct way by a Third-Order nonlinear process, *i.e.* $\omega + \omega + \omega \rightarrow 3\omega$, or by two cascaded Second-Order nonlinear processes, *i.e.* $\omega + \omega \rightarrow 2\omega$ followed by $\omega + 2\omega \rightarrow 3\omega$. The achievement and refinement of such interactions in the framework of guided optics is a current challenge of photonics. The wavelength of the fundamental beam would be preferentially positioned where commercial laser and characterization tools are available such as in the telecom domain around $\lambda_\omega = 1550$ nm. For instance, interesting results of direct THG can be based on mode-matching in silicon waveguides [4,5] or in polycrystal anatase TiO$_2$ [6]. Due to the versatility and high conversion efficiencies of the quasi-phase-matching (QPM) configuration, it is often considered in the case of cascaded THG. Promising results have hence been obtained in planar periodically-poled LiNbO$_3$ (PPLN) waveguides [7] and in ridge waveguides using two PPLN crystals [7,8]. The latter nonlinear micrometric ridge waveguides are emerging due to their high frequency conversion efficiency and good matching with optical fibers [8,9]. Demonstrations have also been realized in ridge waveguides carved in KTP bulk single crystals exploiting birefringence phase-matching (BPM) [10,11] or in QPM periodically-poled KTP [12,13] showing strong performances for second-harmonic generation. Since KTP crystals also exhibit a significant Third-Order nonlinear effect [14], KTP ridge waveguides are appealing for direct THG generation.

In this paper, we report on the first experimental demonstration of direct THG in micrometric KTP ridge waveguides. The BPM conditions is tuned to the chosen wavelengths by tailoring the waveguide transverse dimensions. This study is a preliminary step for designing further quantum optical experiments based on direct Triple Photons Generation (TPG), *i.e.* $3\omega \rightarrow \omega + \omega + \omega$, that is the exact reverse process of THG, thus exhibiting the same BPM conditions [2]. The targeted wavelength for that purpose is $\lambda_{3\omega} = 532$ nm, leading to triplets in the telecom range at $\lambda_{\omega} = 3\lambda_{3\omega} = 1596$ nm.

2. Design of a Y-cut ridge waveguide

The first step is to calculate the BPM conditions as a function of the dimensions of the waveguide in order to design a structure in accordance with the targeted wavelengths. To facilitate light coupling we consider a squared-transverse-section ridge, d being the side of the square. The BPM conditions rely on the wavelength dispersion equations of the effective indices in the considered direction of propagation that is the ridge guide axis. We used the same empirical dispersion equations than those of Ref. [11] relative to the fundamental mode, *i.e.*:

$$neff_i^d(\lambda) = \left(A_i^d \times \lambda^{B_i^d} + \frac{C_i^d}{10^{-6} \times \lambda^{D_i^d} - E_i^d} - F_i^d \times 10^{-6} \times \lambda^{G_i^d} \right)^{H_i^d} + I_i^d \qquad (1)$$

with $i = (x, y, z)$ is relative to the dielectric frame of KTP

The dispersion coefficients $\{A_i^d, B_i^d, C_i^d, D_i^d, E_i^d, F_i^d, G_i^d, H_i^d, I_i^d\}$ depends on the waveguide transverse dimension d and are obtained by fitting discrete values of the effective indices $neff_i$ calculated by COMSOL for different couples (λ, d) in the fundamental transverse mode [11]. These coefficients are given below in Table 1 for $d = 6$ μm, which is very close to the targeted transverse dimension as it will be seen hereafter.

Table 1. Dispersion coefficients of a KTP ridge waveguide of transverse dimension d = 6 μm, at room temperature

i	A_i^d (nm^{-1})	B_i^d	C_i^d (nm)	D_i^d	E_i^d (nm)	F_i^d (nm^{-1})	G_i^d	H_i^d	I_i^d
x	0.4488	0.01948	0.5288	2.277	0.4939	0.88	1.615	0.07128	0.7808
y	1.017	0.004481	1.47	2.323	0.6407	1.242	1.653	0.07207	0.7373
z	2.236	0.006506	0.8399	2.14	0.1814	0.5619	1.811	0.1125	0.7183

Note that Eq. (1) has been established starting from the bulk KTP crystal Sellmeier equations of Ref. [15], which gave a better agreement than using the other main Sellmeier equations of KTP [16,17,18].

From these effective indices data, it has been possible to show that THG can be phase-matched with a Fundamental wavelength around 1600 nm for a propagation along the *y*-axis of the dielectric frame (x, y, z) of KTP. Assuming that both waves in their fundamental transverse mode propagate in the ridge of transverse dimension d, the corresponding BPM relation is:

$$neff_x^d(\lambda_\omega^{BPM}) + 2neff_z^d(\lambda_\omega^{BPM}) - 3neff_x^d(\lambda_{3\omega}^{BPM}) = 0 \qquad (2)$$

The indices x and z stand for the direction of polarization of the waves at the BPM Fundamental wavelength λ_ω^{BPM} or at the third-harmonic $\lambda_{3\omega}^{BPM}$, the corresponding effective indices being $neff_x^d$ or $neff_z^d$. The z-polarization corresponds to the TM_0 mode and the x-polarization to the TE_0 mode.

We calculated λ_ω^{BPM} thanks to Eq. (2) with the effective indices given by Eq. (1) for several discrete values of d. Then we fitted these data by the following empirical equation:

$$\lambda_\omega^{BPM}(d) = \lambda_\omega^{BPM}(\infty) + \rho d^{-\alpha} \qquad (3)$$

where

$$\begin{cases} \lambda_\omega^{BPM}(\infty) = 1476nm \\ \rho = 5945 \\ \alpha = 2.144 \end{cases} \qquad (4)$$

Figure 1 shows the BPM interpolation curve given by Eqs. (3)–(4), where λ_ω^{BPM} is plotted as a function of the transverse dimension of the ridge d.
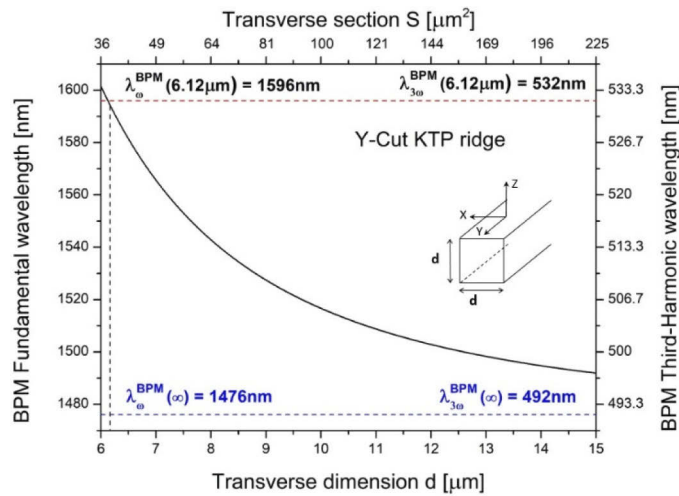

Fig. 1. Calculated BPM THG Fundamental wavelength λ_ω^{BPM} versus the transverse ridge dimension d. The horizontal blue dash line indicates the bulk limit, i.e. $d \rightarrow \infty$, calculated with the refractive indices taken from [14]. The horizontal red dash line corresponds to the targeted BPM wavelengths.

Equation (3) is compatible with the fact that the BPM Fundamental wavelength reaches the value of bulk KTP, *i.e.* $\lambda_\omega^{BPM}(d \rightarrow \infty) = 1476nm$. From Eqs. (3)–(4), it comes that the ridge transverse dimension has to be $d = 6.12\mu m$ in order to get $\lambda_\omega = 1596nm$.

3. Fabrication and geometrical characterization of the waveguide

The general process, similar to the one described in Refs. [11,19], is depicted in Fig. 2. A bulk KTP single crystal provided by Cristal Laser SA whose dimensions are 20 mm along the *x*-axis, 10 mm along the *y*-axis and 500 µm along the *z*-axis is coated on a polished *z*-face with a 600-nm-thick silica layer using inductively-coupled plasma chemical vapor deposition (ICPECVD). This layer is used to provide confinement of light and acts as a cladding, as shown in Fig. 2(a)). A 300-nm-thick gold layer is then sputtered onto the silica as well as onto a high flatness 4 inches diameter silicon wafer (Fig. 2(a)). The KTP sample is then positioned at the center of the silicon wafer so that both metallized faces are brought into contact. Subsequently they are pressed in an EVG wafer bonding machine to form a KTP-silicon heterostructure (Fig. 2(b)). The bonding is realized at room temperature in order to prevent mechanical stress induced by the different thermal coefficients of the materials. The resulting bonding is characterized by an

ultrasound technique which ensures that more than 98% of the surface is bonded [19]. In order to limit the edge effect during the subsequent mechanical thinning, the 500 μm KTP is embedded in a silica matrix (Fig. 2(c)). The KTP-silica structure is then roughly thinned down to 100 μm by surface grinding, followed by a precise grinding and polishing process to be as close as possible to the targeted thickness d=6 μm (Fig. 2(d)).
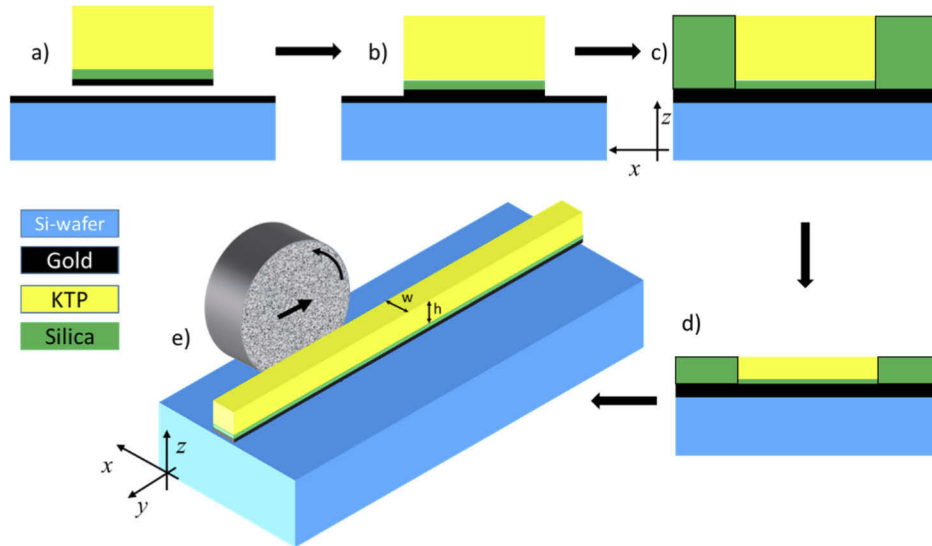

Fig. 2. Chart showing the KTP ridge waveguides fabrication process.

15 ridge waveguides with different widths *w* are then carved in the KTP layer by a precision dicing saw equipped with a 56-mm-diameter and 400-μm-thick diamond blade (Fig. 2(e)). The output and input faces are also diced with the same technique. An average roughness (Ra) of about 2 nm is measured on the top face of the waveguides while Ra is near 5 nm on the diced faces. 40% of the fabricated waveguides are suitable for optical characterizations. The main defects are due to damaged input/output faces attributed to weaker bonding at the edge of the KTP sample. Larger dimensions bulk KTP samples should bring a larger fabrication yield. Waveguides were then analyzed by Scanning Electron Microscopy (SEM), as shown in Fig. 3.
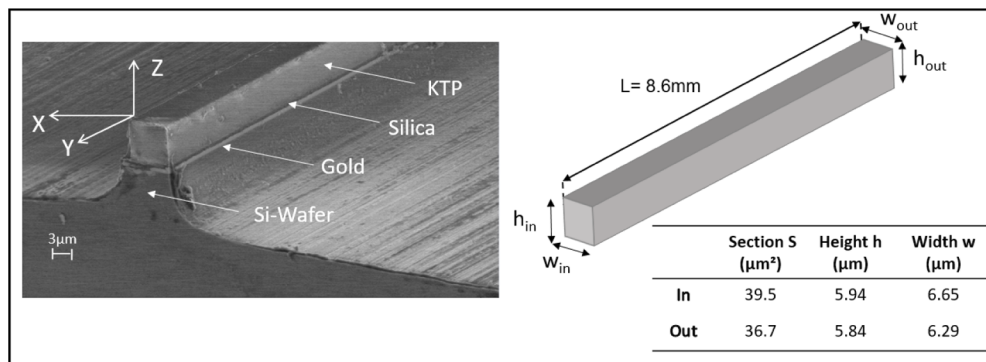

	Section S (μm^2)	Height h (μm)	Width w (μm)
In	39.5	5.94	6.65
Out	36.7	5.84	6.29

Fig. 3. Left: Electron microscopy image of a waveguide. (x, y, z) is the dielectric frame of KTP. Right: Schematic view of the geometrical prismatic shape of the waveguide and dimensions of the input and output faces.

Figure 3 shows that the In and Out sections, *i.e.* S_{in} and S_{out} respectively, are not equal, which is due to the polishing of the upper face as well as to the dicing regarding the two lateral faces. Thus, there is a constant gradient of the transverse section, ranging between $S_{in} = 39.5\,\mu m^2$ and $S_{out} = 36.7\,\mu m^2$. The calculations and analysis of experimental data described in section 4 were performed by considering a "theoretical equivalent" waveguide that has a constant geometry along its axis and with a square transverse section. The square side was then defined by $d_{avg} = \sqrt{(S_{in} + S_{out})/2} = 6.17\mu m$ which is only 50 nm away from the targeted one. The corresponding theoretical BPM Fundamental wavelength calculated according to Fig. 1 or Eqs. (3)–(4) is $\lambda_{\omega}^{BPM} = 1594.2nm$, which is very close to the 1596 nm expected wavelength.

4. BPM wavelengths and spectral acceptance

The experimental investigation of the THG in the above characterized ridge waveguide is carried out using a TOPAS Optical Parametric Generator to deliver the pump beam. Its pulse duration is $\tau_{\omega} = 15ps$, the repetition rate is 10 Hz, and the wavelength is tunable near 1600 nm with an accuracy of ± 1 nm. The polarization is properly adjusted in order to achieve the BPM condition described by Eq. (2). The Fundamental beam is injected in the waveguide using a x20 microscope objective (MO). Proper alignment is made to favor excitation of the fundamental mode of the waveguide as witnessed by the observation of the output light distribution. The generated Third-Harmonic beam is collected by a x40 MO placed at the exit of the waveguide and its energy is measured by a J3S10 Molectron joulemeter. The output Fundamental beam residue is blocked thanks to FGS900M and FGB37 Thorlabs filters. The measured peak intensity of the Third-Harmonic beam plotted as a function of the Fundamental wavelength is shown in Fig. 4.
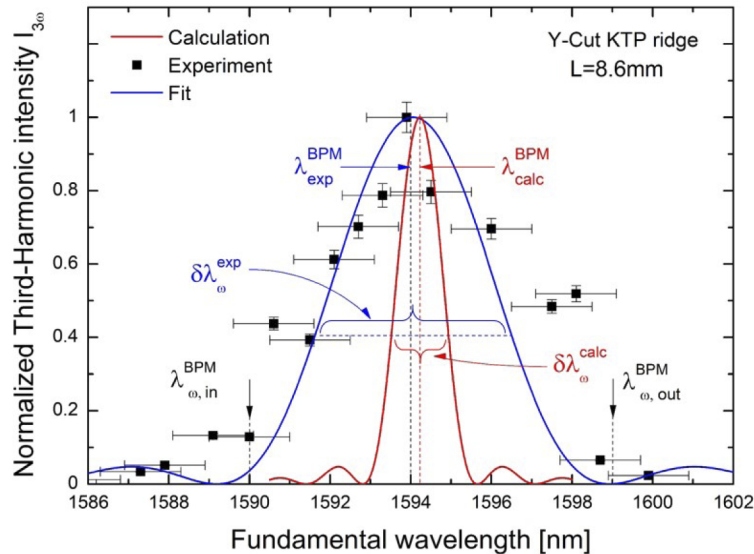

Fig. 4. Normalized intensity of the generated Third-Harmonic beam as a function of the Fundamental wavelength. The black squares are experimental data. The pump intensity is fixed at 0.4 GW.cm^{-2}. The red curve corresponds to the calculation in the case of a perfectly uniform 8.6 mm long square ridge with a side $d_{avg} = 6.17\,\mu m$. The blue curve is a sinc^2 fit. The vertical dashed lines indicate the BPM Fundamental wavelengths, $\lambda_{\omega,in}^{BPM}$ and $\lambda_{\omega,out}^{BPM}$ corresponding to the measured transverse sections S_{in} and S_{out}, respectively. The bandwidths $\delta\lambda_{\omega}^{exp} = 4.75nm$ and $\delta\lambda_{\omega}^{calc} = 1.5nm$ are measured at 0.405 of the maxima.

Figure 4 shows that the BPM Fundamental wavelength is measured at $\lambda_\omega^{BPM} = 1594nm$. It is very close to the value predicted by Eq. (3), *i.e.* $\lambda_\omega^{BPM} = 1594.2nm$, which validates our approximation of the ridge shape by a parallelepiped with an average square transverse section. It would have been necessary to take into account the exact geometry if the deviation to a square section had been larger.

Concerning their full widths at 0.405 of the maxima, the calculation gives a value $\delta\lambda_\omega^{calc} = 1.5nm$ which is smaller than the measured value $\delta\lambda_\omega^{exp} = 4.75nm$ by more than a factor of three. This difference is well explained by the prismatic shape of the waveguides. Actually, there is a gradual change of the transverse sections, the extremal values being $S_{in} = 39.5\mu m^2$ and $S_{out} = 36.7\mu m^2$ according to Fig. 3. The consequence is a corresponding gradient of effective indices leading to a change of phase-matching conditions. Figure 4 shows that the values of the bandwidths corresponding to S_{in} and S_{out}, *i.e.* $\lambda_{\omega,in}^{BPM} = 1590nm$ and $\lambda_{\omega,out}^{BPM} = 1599nm$ respectively, well frame the phase-matching peak at 1594 nm. These data well illustrate the fact that a variation in the waveguide dimension can influence the phase-matching conditions [20].

All these good agreements validate our calculation of the effective indices as well as the fact that the experiments have been achieved in the fundamental mode for both the ω and 3ω waves.

5.   Conversion efficiency

Figure 5 shows the Third-Harmonic energy measured at the exit of the KTP ridge as a function of the incoming Fundamental energy, both energies being measured by a J3S10 Molectron joulemeter.
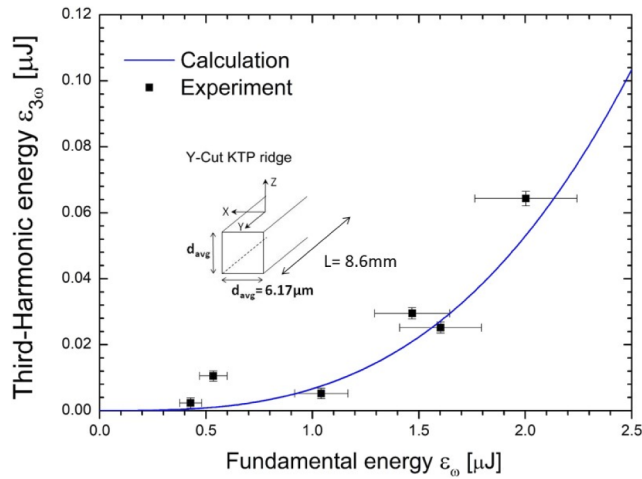

Fig. 5. Measured Third-Harmonic energy (black square) at the exit of the crystal as a function of the Fundamental energy at the entrance. Calculated energy (blue curve) without any adjusting parameter.

The energy conversion efficiency reaches up to 3.4% for a Fundamental energy as low as 2 μJ. This energy has not been exceeded in order to avoid any damage to the waveguide.

The theoretical prediction of the conversion efficiency fully matches the experimental results without any fitting parameters, as shown in Fig. 5. The calculations were performed in the undepleted pump approximation (UPA) starting from the following relation that expresses the first derivative of the complex amplitude of the Third-Harmonic electric field $E_{3\omega}^x$ as function of the two components of the Fundamental complex electric field E_ω^x and E_ω^z where indices x and z stand for the orientations of the polarization in the dielectric frame, the waves propagating in the

y-axis:

$$\frac{\partial E_{3\omega}^x(y)}{\partial y} = j\frac{\pi}{n_{eff_x}(3\omega)\lambda_{3\omega}}\chi_{16}^{(3)}(3\omega)E_\omega^x(y)E_\omega^z(y)E_\omega^z(y) \tag{5}$$

where $\chi_{16}^{(3)}$ is the excited Third-Order nonlinear coefficient [14].

Even under the UPA, the Fundamental amplitudes are taken with a possible variation as a function of *y* in order to take into account the propagation losses, *i.e.*:

$$E_\omega^{x,z}(y) = E_\omega^{x,z}(0)\sqrt{\exp(-\beta_\omega y)} \tag{6}$$

where β_ω is the loss coefficient at the Fundamental wavelength.

To take into account the longitudinal gradient of the phase-matching conditions due to the change of the transverse section of the KTP ridge, calculation has been achieved through the introduction of an effective interaction length, denoted L_{eff}. This parameter can be directly deduced from the widths of the calculated and experimental phase-matching curves shown in Fig. 4. Indeed, the product between the interaction length by the bandwidth of the phase-matching peak has to be a constant quantity [21]. It is then straightforward to deduce an effective length $L_{eff} = L.(\delta\lambda_\omega^{calc}/\delta\lambda_\omega^{\exp}) = 2.7mm$, where $L = 8.6mm$ is the geometrical length of the KTP ridge. It appears that the effective length is about 1/3 smaller than the geometrical length, which reflects the fact that the mismatch between the nonlinear polarization and the Third-Harmonic wave varies as a function of the longitudinal coordinate *y*.

Equation (6) inserted in Eq. (5) followed by its integration over L_{eff} leads to the following relation:

$$E_{3\omega}^x(L_{eff}) = j\Omega\Gamma L_{eff}E_\omega^x(0)[E_\omega^z(0)]^2 \tag{7}$$

with Ω and Γ defined as

$$\begin{cases} \Omega = \frac{\pi}{neff_x(3\omega)\lambda_{3\omega}}\chi_{16}^{(3)}(3\omega) \\ \Gamma = \sqrt{\exp(-\beta_{3\omega}L_{eff})}\int\limits_0^{L_{eff}}[\exp(-\beta_\omega y)]^{3/2}dy \\ = \frac{2}{3}\sqrt{\exp(-\beta_{3\omega}L_{eff})}\left[\frac{1-\exp(-3\beta_\omega L_{eff}/2)}{\beta_\omega}\right] \end{cases} \tag{8}$$

where $\beta_{3\omega}$ is the propagation loss coefficient at the Third-Harmonic wavelength.

Finally, the Third-Harmonic energy is:

$$\varepsilon_{3\omega}(L_{eff}) = \frac{103}{3\pi^3\sqrt{3}}\frac{\mu_0}{\varepsilon_0}\frac{(T_\omega^z)^2 T_\omega^x T_{3\omega}^x}{(\tau_\omega W_\omega^2)^2}\frac{\Omega^2}{n_{eff,\omega}^x(n_{eff,3\omega}^z)^2}\Gamma^2[\varepsilon_\omega(0)]^3 \tag{9}$$

where $T_{\omega,3\omega}^{x,z} = 4n^{x,z}(\omega,3\omega)/[1+n^{x,z}(\omega,3\omega)]^2$ are the Fresnel transmissions coefficient, W_ω is the 1/e² mode radius, and $\varepsilon_\omega(0)$ is the Fundamental incident energy. The numerical values of the parameters used in the calculation are summed up in Table 2.

Table 2. Parameters used in the calculation of the generated Third-Harmonic energy. The nonlinear coefficient $\chi_{16}^{(3)}$, and the principal refractive indices n^x and n^z are calculated from [14].

	λ [nm]	$\chi_{16}^{(3)}$[m²V⁻²]	τ [ps]	W [µm]	Tᶻ	Tˣ	β [cm⁻¹]	nˣ	nᶻ
ω	1594	-	15	2.5	0.92	0.93	0.3	1.7205	1.8067
3ω	531.3	8.05.10⁻²²	-	-	-	0.92	0.1	1.7780	-

The propagation loss coefficients $\beta_{\omega,3\omega}$ and Fundamental mode radius W_ω are calculated from Rsoft simulations. It also reveals than the losses mainly come from the presence of the gold layer below the silica buffer layer. Improved structures with a thicker buffer layer are planned.

As mentioned in section 4 about phase-matching, the previous calculations of generated intensity are in perfect agreement with the measurements by assuming that the Fundamental and Third-Harmonic waves are in the fundamental waveguide modes. This accordance validates this assumption of a single and fundamental mode operation, for which the overlap between the interacting waves is maximal.

6. Conclusions

In summary, we have shown that KTP ridge waveguides are good candidates for efficient phase-matched THG of which we made the first experimental demonstration. Tailoring waveguide dimensions enables birefringence phase-matching at telecom wavelengths. A 8.6-mm-long ridge waveguide based on a single KTP crystal allowing THG to be phase-matched at 1594 nm has been fabricated. We obtained an energy conversion efficiency of 3.4% for a fundamental energy of 2 µJ in the picosecond regime. The THG conversion efficiency can be optimized by improving the waveguide cross section uniformity and by decreasing the propagation losses. The later will be done by increasing the thickness of the silica buffer layer between the gold film and the KTP crystal. The fabrication of samples with a 2-µm-thick silica layer is in progress with the target to reach a THG conversion efficiency up to 50%, which would be a record for direct THG. Such an efficiency would be at the best level compared with commercially available sources, knowing that the later ones are systematically based on Second-Order cascaded THG and so are more complex to setup.

The full agreement between calculation and measurement validates our calculation of effective indices as well as the notion of effective interaction length for modeling the nonlinear effect along the unperfect ridge waveguide.

This study of BPM THG ($\omega + \omega + \omega \rightarrow 3\omega$) paves the way for an optimal design of TPG ($3\omega \rightarrow \omega + \omega + \omega$) experiments. Using a reliable quantum model [22] and assuming no losses due to evanescent waves, *i.e.* with 2-µm-thick silica layer, we expect to generate up to 100 triplets per second at $\lambda_\omega = 1596$ nm in a 5-cm-long KTP ridge waveguide pumped with 5 W at $\lambda_{3\omega} = 532$ nm in the CW regime. A new quantum information frontier is foreseen.

References

1. K. Banaszek and P. L. Knight, "Quantum interference in three-photon down conversion," Phys. Rev. A **55**(3), 2368–2375 (1997).
2. K. Bencheikh, F. Gravier, J. Douady, J. A. Levenson, and B. Boulanger, "Triple photons: a challenge in nonlinear and quantum optics," Comptes Rendus Physique **8**(2), 206–220 (2007).
3. V. Ansari, E. Roccia, M. Santandrea, M. Doostdar, C. Eigner, L. Padberg, I. Gianani, M. Sbroscia, J. M. Donohue, L. Mancino, M. Barbieri, and C. Silberhorn, "Heralded generation of high-purity ultrashort single photons in programmable temporal shapes," Opt. Express **26**(3), 2764–2774 (2018).
4. B. Corcoran, C. Monat, C. Grillet, D. J. Moss, B. J. Eggleton, T. P. White, L. O'Faolain, and T. F. Krauss, "Green light emission in silicon through slow-light enhanced third harmonic generation in photonic crystal waveguides," Nat. Photonics **3**(4), 206–210 (2009).
5. S. Sedeberg, C. J. Firby, and A. Y. Elezzabi, "Efficient broadband third-harmonic generation in silicon nanophotonic waveguides spectrally shaped by nonlinear propagation," Opt. Express **27**(4), 4990–5004 (2019).
6. C. C. Evans, K. Shtyrkova, O. Reshef, M. Moebius, J. D. B. Bradley, S. Griesse-Nascimento, E. Ippen, and E. Mazur, "Multimode phase-matched third harmonic generation in sub-micrometer-wide anatase TiO_2 waveguides," Opt. Express **23**(6), 7832–7841 (2015).
7. K. Kintaka, M. Fujimara, T. Suhara, and H. Nishihara, "Third harmonic generation of Nd:YAG laser light in periodically poled $LiNbO_3$ waveguide," Electron. Lett. **33**(17), 1459–1461 (1997).

8. V. Pecheur, H. Porte, J. Hauden, F. Bassignot, M. Deroh, and M. Chauvet, "Watt-level SHG in undoped high step-index PPLN ridge waveguides," OSA Continuum **4**(5), 1404–1414 (2021).

9. L. G. Carpenter, S. A. Berry, A. C. Gray, J. C. Gates, P. G. R. Smith, and C. B. E. Gawith, "CW demonstration of SHG spectral narrowing in a PPLN waveguide generating 2.5 w at 780 nm," Opt. Express **28**(15), 21382 (2020).

10. C. Chen, C. E. Rüter, M. F. Volk, C. Chen, Z. Shang, Q. Lu, S. Akhmadaliev, S. Zhou, F. Chen, and D. Kip, "Second harmonic generation of diamond-blade diced KTiOPO4 ridge waveguides," Opt. Express **24**(15), 16434 (2016).

11. V. Boutou, A. Vernay, C. Felix, F. Bassignot, M. Chauvet, D. Lupinski, and B. Boulanger, "Phase-matched second-harmonic generation in a flux grown KTP crystal ridge optical waveguide," Opt. Lett. **43**(15), 3770–3773 (2018).

12. C. C. Kores, P. Mutter, H. Kianirad, C. Canalias, and F. Laurell, "Quasi-phase matched second harmonic generation in periodically poled Rb-doped KTiOPO$_4$ ridge waveguide," Opt. Express **26**(25), 33142–33147 (2018).

13. C. Eignier, M. Santandrea, L. Padberg, M. F. Volk, C. E. Rüter, H. Herrmann, D. Kip, and C. Silberhorn, "Periodically poled ridge waveguides in KTP for second harmonic generation in the UV regime," Opt. Express **26**(22), 28827–28833 (2018).

14. B. Boulanger, J. P. Fève, P. Delarue, I. Rousseau, and G. Marnier, "Cubic optical nonlinearity of KTiOPO4," J. Phys. B: At., Mol. Opt. Phys. **32**(2), 475–488 (1999).

15. K. Kato, "Parametric Oscillation at 3.2 pm in KTP Pumped at 1.064 pm," J. Quantum Electron. **27**(5), 1137–1140 (1991).

16. B. Boulanger, J. P. Fève, G. Marnier, C. Bonnin, P. Villeval, and J. J. Zondy, "Absolute measurement of quadratic nonlinearities from phase-matched second-harmonic generation in a single KTP crystal cut as a sphere," J. Opt. Soc. Am. B **14**(6), 1380–1386 (1997).

17. K. Fradkin, A. Arie, A. Skliar, and G. Rosenman, "Tunable midinfrared source by difference frequency generation in bulk periodically poled KTiOPO$_4$," Appl. Phys. Lett. **74**(7), 914–916 (1999).

18. S. Emanueli and A. Arie, "Temperature-dependent dispersion equations for KTiOPO4 and KTiOAsO4," Appl. Opt. **42**(33), 6661–6665 (2003).

19. M. Chauvet, F. Henrot, F. Bassignot, F. Devaux, L. Gauthier-Manuel, V. Pecheur, H. Maillotte, and B. Dahmani, "High efficiency frequency doubling in fully diced LiNbO$_3$ ridge waveguides on silicon," J. Opt. (United Kingdom **18**(5), 085503 (2016).

20. M. Santandrea, M. Stefszky, G. Roeland, and C. Silberhorn, "Characterisation of fabrication inhomogeneities in Ti:LiNbO3 waveguides," New J. Phys. **21**(12), 123005 (2019).

21. B. Boulanger and J. Zyss, "Non-linear Optical properties," Chapter 1.7 in International Tables for Crystallography, Vol. D: Physical Properties of Crystals, A. Authier Ed., International Union of Crystallography, Kluwer Academic Publisher, Dordrecht, Netherlands, 181–222 (2013).

22. A. Dot, A. Borne, B. Boulanger, K. Bencheikh, and J. A. Levenson, "Quantum theory analysis of triple photons generated by a χ(3) process," Phys. Rev. A **85**(2), 023809 (2012).